Pratidhwani the Echo
A Peer-Reviewed International Journal of Humanities & Social Science
ISSN: 2278-5264 (Online) 2321-9319 (Print)
***Impact Factor: 6.28** (Index Copernicus International)*
Volume-XI, Special Issue, June 2023, Page No.296-305
Published by Dept. of Bengali, Karimganj College, Karimganj, Assam, India
Website: http://www.thecho.in

Synthesis and Characterization Techniques of Composite Thermoelectric (TE) Materials: A Review

Mr. Babai Patra
State Aided College Teacher, Dept. of Physics, Panchmura Mahavidyalaya, Bankura, West Bengal, India

Abstract:
Thermoelectric materials and devices, which can convert heat energy to electrical power, provide opportunities to harvest useful electricity from waste heat. Because of the advantages of no moving parts, no noise signature, and exceptional reliability, TE conversion technology is widely used in power generation and refrigeration. The purpose of this paper to give an idea about synthesis and characterization techniques of composite TE materials that is used in different type of research work. Also, the current applications of TE materials and their devices are reviewed. Lastly, the future development of highly efficient TE materials through synergetic optimization and their future applications will be proposed.

Keywords: Thermoelectric materials, ZT, Synthesis, Characterization, Applications.

Introduction: Due to the pressing need to shift the world energy matrix towards cleaner and renewable energy sources, the search for materials that present high thermoelectric conversion efficiency has intensified in recent years. A thermoelectric converter requires two thermoelectric materials, one with n-type charge carriers and the other p-type.[1] The development of better thermoelectric conversion devices has deserved special attention because of favourable aspects such as high scalability, absence of moving parts, elimination of chlorofluorocarbons, reuse of waste heat from automobiles and other machines, and improvement of energy sources for space probes. A thermoelectric converter is a heat converter and as such obeys all the laws of thermodynamics. A common misconception is to think that a heat converter has the same characteristics as a heat engine. A heat engine converts temperature differences into mechanical power, whereas a heat converter transforms temperature differences directly into electricity.

TE materials play an increasingly crucial part in sustainable development. The energy conversion efficiency of a TE material is mainly depicted by its dimensionless figure of merit $ZT = \sigma S^2T/\kappa$, where σ, S, T and κ are the electrical conductivity, Seebeck coefficient, absolute temperature and thermal conductivity, respectively. [2, 3] To achieve high ZT value, a large power factor ($S^2\sigma$) and/or low κ should be secured, in which a large $S^2\sigma$ implies the high heat-electricity conversion efficiency of charge carriers while a low κ indicates the

ability of remaining the suitable temperature gradient.[4] The current ZT values of the thermoelectric materials are lies between 1 and 2.[5] Resulting in that the current thermoelectric energy conversion efficiency is comparable to the other energy conversion technologies, such as photovoltaic cells and solar thermal plants.[6] Considerable research has been continuing to further drive ZT higher than 2 with the predicted efficiency over 20%, [7, 8] which can attract highly exciting prospect in the energy generation and conservation fields.

In term of the industrial and automotive applications, waste-heats are generally produced in the temperature range of (500 - 900 K). [9-11] to recover such waste heats, developing of high performance mid-temperature (400 - 900 K) thermoelectric materials is highly desired. It is still urgently needed to improve ZT of TE materials. Based on the fundamental understandings on TEs, tremendous efforts have been devoted to achieve ZT > 2, such as in Bi_2Te_3/Sb_2Te_3 superlattice, [12] PbTe, [13] SnSe, [14] and Cu_2Se [15].

In this review, we firstly highlighted the key strategies to synthesis process of some composite TE materials and their thermoelectric performance and then we proposed the future development of these composite TE materials associated structures through synergetic optimization, which will guide and inspire researchers to explore advanced composite based thermoelectric materials.

Synthesis: In this section briefly discussed different techniques which are adopted and employed to synthesize of composite TE materials.

Material synthesis techniques: The hydrothermal/solvothermal method is employed for the synthesis of bismuth selenide, lead telluride, and cobalt antimony skutterudite and ball milling technique is used for the synthesis of Bi-Sb alloy.

Hydrothermal/solvothermal method: Solv thermal or hydrothermal technique has been proposed as one of the efficient methods for the large-scale synthesis of nanostructured materials. It has been employed to synthesize various kinds of semiconducting materials including thermoelectric materials with different morphologies and sizes from large ingots to nanostructures [1, 2]. In a typical synthesis process, starting materials in the specific end-product stoichiometry were mixed with reductant and/or pH controlling agent in the presence of either a solvent (for the solvothermal route) or an aqueous solution (for the hydrothermal route). A schematic of the hydrothermal/solvothermal technique employed for nanomaterial synthesis. In this review work, different kinds of organic solvents including ethanol, dimethyl formamide (DMF), ethylene glycol (EG), and inorganic solutions including a water/glycerol mixture were used as the solvent for solvothermal synthesis and water was used as the solvent for hydrothermal synthesis. Sodium borohydride ($NaBH_4$) and sodium hydroxide (NaOH) were used as reductant and pH controlling agent, respectively.

.

Ball milling method: Recently, the ball milling process has been developed as one of the widely used techniques for the synthesis of nanostructured thermoelectric materials [42, 43].

During the ball milling process, mechanical alloying and nanostructuring occurs simultaneously through a sequence of collision events inside a high energy ball mill [44]. In a typical ball milling process, elemental chunks or powders of precursor materials in the specific resulting alloy stoichiometry were placed inside a ball mill jar containing stainless steel balls. The whole process was operated inside an argon filled glove box to reduce the possibility of oxidation of rather reactive precursor materials. The ball mill jar was then placed in a high energy ball mill machine. The ball milling process has several advantages such as highly scalable yield up to kilograms of material in a few hours. The ball milled nanomaterials are easy to sinter to form high density pellets with a large number of grain boundaries, which is favourable for increasing the Seebeck coefficient and decreasing the thermal conductivity to optimize the power factor.

Bridgman technique: The Bridgman technique requires a two-zone furnace. The materials which melt congruently do not decompose before melting and those do not undergo phase transformation between the melting point and room temperature can be grown as single crystal by Bridgman technique. The material to be grown is encapsulated in glass or quartz tube and suspended in the furnace having suitable gradient for growth. The tip of the ampoule is mainly conical shaped to enhance nucleation of a single crystal.

Although there are so many techniques apart from these techniques, some different type of techniques are shown in the table below.

Table 1. Thermoelectric properties of the highest performing Composite TE materials at a stated temperature (T). κ is the thermal conductivity.

Materials	**Carrier type**	**T (K)**	**κ**	***ZT***	**Synthesis method***	**Ref.**
SnSe Single Crystal	p	923	0.34	2.60	Bridgman method	[15]
$PbTe_{0.85}Se_{0.15}$-2%Na-4%SrTe	p	923	0.85	2.30	Melting-SPS	[16
Sr-PbSe	p	900	0.80	1.50	Melting-HP	[17]
PbTe/PbSe nanoparticles	n	623	0.90	1.85	SBR-SPS	[18]
Na-doped $(PbTe)_{0.65}(PbS)_{0.25}(PbSe)_{0.1}$	p	850	1.00	2.00	MAG-SPS	[19]
$AgPb_mSbTe_{m+2}$	n	723	0.77	1.54	BM-SPS	[20]
$Tl_{0.02}Pb_{0.98}TeSi_{0.02}Na_{0.02}$	p	770	1.00	1.70	BM- HP	[21]
PbTe–CdTe alloy	p	775	1.30	1.70	MAG-HP	[22]
Cu_2Se	p	1000	0.65	1.80	SHS-SPS	[23]
$Cu_2S_{0.52}Te_{0.48}$	p	1000	0.50	2.10	SSR-SPS	[24]

**SPS = spark plasma sintering; HP = hot press; BM = ball milling; SSR = solid state reaction; SBR = Solution-based reaction; MAG: melting, annealing and grounding; SHS = self-propagating high-temperature synthesis; the κ values are corresponding to the peak ZT values, and this unit is* $Wm^{-1}K^{-1}$. [45]

Characterization: In this section briefly discuss about different types of techniques which are employed to characterise and measure the transport properties of composite TE materials.

Examination techniques for structural characterization:

X-ray diffraction (XRD): An x-ray diffraction (XRD) technique was used to identify the phase of the nanocrystals and to get the information on the crystal structure. The XRD measurement was carried out using a diffractometer equipped with a Cu anode. The XRD patterns were collected with a step size of 0.01º and a scan rate of 1 sec/step. The intensity of X-rays diffracted by the sample was constantly recorded as the detector and the sample were rotated by respective angles. A peak in intensity occurs at an angle θ when the sample contains lattice planes with d-spacings that diffract X-rays at that value of θ. Finally, the result was presented as peaks at 2θ on the x-axis and intensity of X-ray on the y-axis. The XRD pattern, thus obtained was compared to the standard XRD profiles of different materials that are available from International Center for Diffraction Data as the Powder Diffraction File (PDF), commonly known as a JCPDS file. Unit cell parameters could be calculated after indexing each reflection peak to corresponding hkl (Miller indices) values.

Scanning electron microscopy (SEM): A field emission scanning electron microscope (SEM) was used to analyze the surface morphology of nanocrystals. In SEM, a high-energy beam of electrons interacts with the atoms inside the sample generating signals that consist of the information about the morphology of the sample. Surface morphology analysis of the sample was performed by JEOL JSM-6330F SEM, which was operated at a15kV accelerating voltage 43 and gives magnifications up to 500k. To prepare a sample for SEM measurement, the powder sample was ultrasonicated in alcohol for 30 minutes. A very small drop of sample solution was dropped onto silicon substrate and the alcohol was allowed to evaporate. Most of the time, the sample was coated with gold film to make it conductive to get a better SEM image.

Transmission electron microscopy (TEM): The structural analysis of the nanostructures was carried out by a transmission emission microscope (TEM). Transmission emission microscope works on the principle that an electron can behave as a wave (de Broglie hypothesis). Smaller de Broglie wavelengths of electrons, which are on the order of spacing of atoms, enable TEM to image atoms at significantly higher resolution. The electrons generated thermionically and accelerated with an accelerating voltage transmit through the sample and the transmitted beam is used to form the image. The images are of various types such as low magnification TEM, high resolution TEM (HRTEM), selected area diffraction (SAED) pattern, and electron dispersive X-ray spectroscopy (EDS). The HRTEM images

provide the information about the phase of the crystal, and SAED patterns give the information about the crystallinity of sample.

Laser-induced breakdown spectroscopy (LIBS): In the review work, LIBS was used to detect the very small content of elements such as indium doping in the PbTe matrix and ytterbium filling in the $CoSb_3$ structure. Equipped with a highly energetic laser as an excitation source, LIBS works on the principle of atomic emission spectra. When the laser beam strikes the sample, it initiates highly energetic luminous plasma from the ablated sample mass, which consists of free electrons, excited atoms, and ions. A typical plasma spectrum is a signature of the chemical species in the sample and provides information about the chemical species composition and relative abundance. [25]

Transport property measurement techniques: Electrical conductivity (σ), Seebeck coefficient (S), and thermal conductivity (κ) are the fundamental transport properties that characterize the efficiency of a thermoelectric material. Electrical conductivity and Seebeck coefficients were measured by commercial equipment, Ulvac ZEM 3 and thermal conductivity was measured using a laser flash system (Netzsch LFA 457).

Electrical conductivity and Seebeck coefficient measurement: Figure 1 shows the measurement system that was used to measure the electrical properties of the samples. Figure 1 (a) displays the photograph of the commercial ZEM-3 system and Fig. 1 (b) shows a sample mounted in the ZEM-3 apparatus for electrical resistivity and Seebeck coefficient measurement. In the ZEM-3 system, electrical resistivity was measured using a four probe technique and electrical conductivity was calculated from the electrical resistivity. The four probe technique for measuring the resistivity simply accounts for the contact resistance between metal electrodes and the semiconducting samples. Figure 2 (a) displays a schematic diagram of the four probe used by the ZEM-3 system. As shown in Fig. 2 (a), in the four probe technique current I was passed through one set of probes (blue blocks) and the voltage

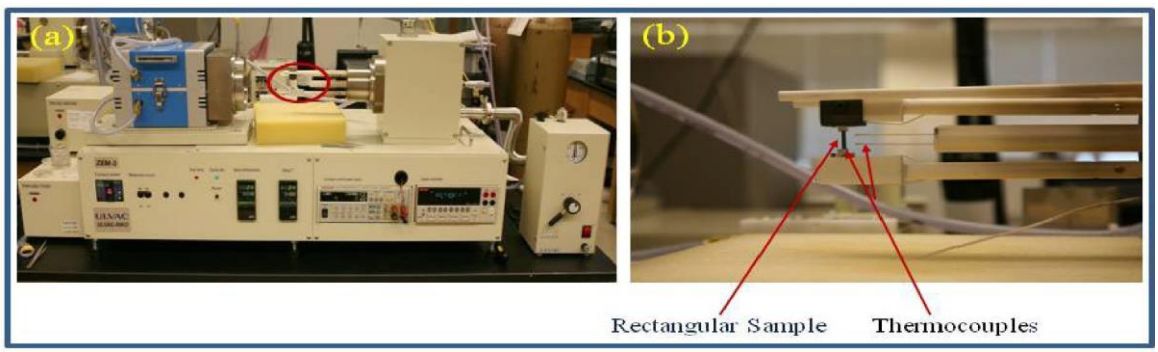

Figure 1 a) A commercial ZEM-3 system, and b) magnified sample holder region (indicated by red circle in (a)) with a sample mounted for measurement, courtesy Prof. Zhifeng Ren's lab (University of Houston). [26]

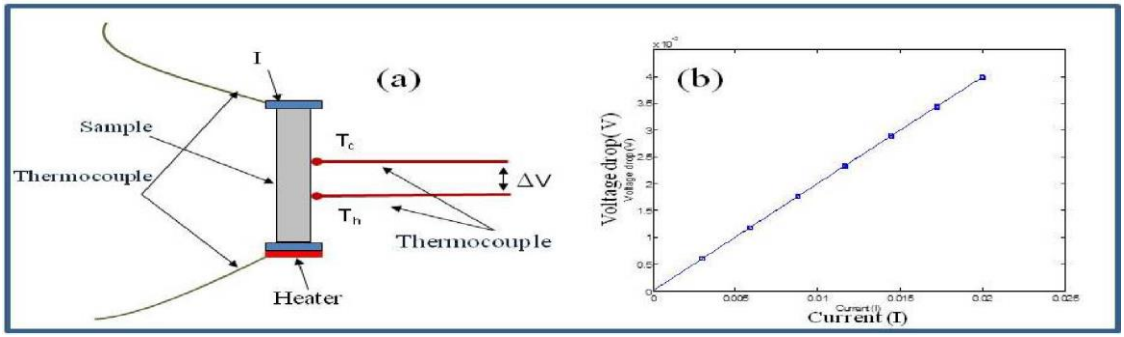

Figure 2 a) Schematic diagram of four probe technique in ZEM-3 system, and b) a typical I-V curve for resistance measurement. [26]

Difference (ΔV) was measured using another set of probes (small red spheres). These four probes were connected to four thermocouples. The voltage and current control, data acquisition, and interpretation were fully automated and computer controlled. The electrical resistivity was found from the relation $\rho = \frac{A}{l}\left(\frac{\Delta V}{\Delta l}\right)$, where (ΔV/ΔI) is the slope of the I-V curve as shown in Fig. 2 (b), A is the cross-sectional area of the sample and l is the distance between the voltage probes. The electrical conductivity was then calculated as the reciprocal of the resistivity. During the resistivity measurement, the temperatures at both probes were kept constant to minimize the Seebeck voltage.

The same ZEM-3 system (Fig. 1) was used for Seebeck coefficient measurement. The Seebeck coefficient is simply defined as the ratio of an open-circuit potential difference (ΔV) to a temperature gradient (ΔT), $S = \frac{\Delta V}{\Delta T}$

For See beck coefficient measurement, the voltage and temperatures were measured simultaneously by the same thermocouple probe (small red spheres) as shown in Fig. 2 (a). Then, the voltage difference (ΔV) was measured for a set of temperature differences (ΔT) between the two probes and the See beck coefficient was calculated from the slope of ΔV-ΔT plot.

Thermal conductivity measurement: A laser flash technique was used to measure the thermal conductivity of the samples in the review work. In the laser flash technique, thermal conductivity was calculated using the relation, $\kappa = C\alpha\rho$, where C is specific heat capacity, α is the thermal diffusivity, and ρ is the density of the sample. A laser flash system (Nestzsch LFA 457) was used to measure α and C, and Archimedes' principle was used to measure ρ of the material. A Nestzsch LFA 457 system (shown in Fig. 3 (a)) can measure α and C from room temperature to 950^{o}C.

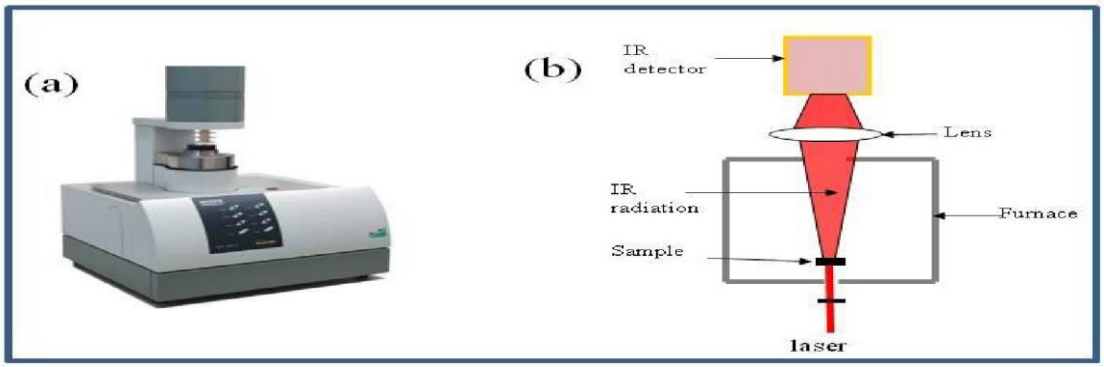

Figure 3 a) A laser flash system (Nestzsch LFA 457), courtesy Prof. Zhifeng Ren's lab (University of Houston) and b) schematic diagram of the laser flash technique [26]

The laser flash system used a disk of diameter 12.7 mm and thickness ranging from 1-2 mm. All samples, together with the reference sample needed for specific heat calculation were graphite coated to match the absorptivity and emissivity that is specifically important for specific heat calculation. The samples were then placed with one side facing the laser beam and the other side facing an Indium Antimonide (InSb) IR detector inside an argon-environment furnace as shown in Fig. 3 (b). A heater was used to adjust the furnace temperature as needed for temperature dependent diffusivity and specific heat measurement. A laser beam struck the front sample surface causing a heat pulse to travel through the sample's thickness. The actual IR signal was detected by the IR detector on the other side of the system and transferred the required data for the measurement of α and C to the computer. The equipment was fully automated and controlled to record, analyze, and interpret the data of thermal diffusivity and specific heat capacity. Then thermal conductivity was calculated using equation.

Application: TE devices[27, 28] have long been applied as they can achieve solid state power generation or refrigeration without any noise or vibration, showing many advantages such as high sensitivity to temperature change[28,29] and emission-free operation. Such features become huge advantages when TE materials are utilized in various fields such as remote power supply (Radioisotope thermoelectric generators, RTGs),[30,31] automotives, [32-35] temperature sensors[36] and control devices,[28,37] water condensation[38] and implantable/wearable devices.[39-,40,41] Up to now, significant progress has been made in developing high performance TE devices.

Future Scope: The rapid development of TE materials and devices has piqued the interest of many people because of their enormous potential in applications such as next-generation power generators, self-powered wearable electronics, and power supplies for different externally powered portable devices. Composite TE material based conducting materials have appealing ultralow thermal conductivity, light weight, and tuneable Seebeck coefficient, making them a very promising choice for heat-to-electricity conversion. In this review, we explored the most recent developments in composite TE material, including the

key ingredients, production method, TE performance, and variables influencing TE performance and the associated mechanisms. Although tremendous progress was made in the field of TE material, research in this sector is still in its infancy, especially when compared to organic or inorganic based TE films or bulks. The following elements of TE material and related devices might be the subject of future study.

It remains a significant challenge for 3D composite TE materials to concurrently enhance S while reducing/maintaining low thermal conductivity, especially when compared to equivalent TE films. To optimize the preparation and TE performance of composite TE materials, optimization methods (doping, de-doping, pre-/post treatment), morphology and structure control (1D nanowires or nanotubes, 2D Nano sheets), and enhancement mechanisms (synergistic effect, energy filtering effect, phonon scattering effect) of selected films or bulk materials with high TE properties can be used. Furthermore, high elasticity and/or flexibility can be used to make compressible and/or elastic TE devices.

Acknowledgement: B.P. expresses sincere gratitude to Dr. Anal Biswas, Principal of Panchmura Mahavidyalaya and Dr. Arpita Bhowmick, IQAC coordinator of Panchmura Mahavidyalaya for providing this wonderful opportunity to work. The completion of the work would not have been possible without their help and insights.

Reference:

1. D.M. Rowe, Thermoelectric Handbook: Macro to Nano, CRC Press, Boca Raton, FL, 2006.
2. Poudeu, P.F.P.; Guéguen, A.; Wu, C.-I.; Hogan, T.; Kanatzidis, M.G. High Figure of Merit in Nanostructured n-Type KPb_mSbTe_{m+2} Thermoelectric Materials. Chem. Mater. 2010, 22, 1046–1053.
3. Snyder, G.J.; Toberer, E.S. Complex thermoelectric materials. Nat. Mater. 2008, 7, 105–114.
4. G.J. Snyder, E.S. Toberer, Nat. Mater. 2008, 7, 105.
5. Y. Pei, X. Shi, A. LaLonde, H. Wang, L. Chen, G.J. Snyder, Nature 2011, 473, 66.
6. M. Zebarjadi, K. Esfarjani, M.S. Dresselhaus, Z.F. Ren, G. Chen, Energy Environ. Sci. 2012, 5, 5147.
7. H. Liu, X. Yuan, P. Lu, X. Shi, F. Xu, Y. He, Y. Tang, S. Bai, W. Zhang, L. Chen, Y. Lin, L. Shi, H. Lin, X. Gao, X. Zhang, H. Chi, C. Uher, Adv. Mater. 2013, 25, 6607.
8. L.-D. Zhao, S.-H. Lo, Y. Zhang, H. Sun, G. Tan, C. Uher, C. Wolverton, V.P. Dravid, M.G. Kanatzidis, Nature 2014, 508, 373.
9. C.-T. Hsu, G.-Y. Huang, H.-S. Chu, B. Yu, D.-J. Yao, Appl. Energ. 2011, 88, 1291.
10. T.D. Barr, F.A. Dahlen, J. Geophys. Res. Solid Earth 1989, 94, 3923.
11. L. Yang, Z.-G. Chen, M. Hong, L. Wang, D. Kong, L. Huang, G. Han, Y. Zou, M. Dargusch, J. Zou, Nano Energy 2017, 31, 105.
12. R. Venkatasubramanian, E. Siivola, T. Colpitts, B. O'Quinn, Nature 2001, 413, 597.

13. K. Biswas, J. Q. He, I. D. Blum, C. I. Wu, T. P. Hogan, D. N. Seidman, V. P. Dravid, M. G. Kanatzidis, Nature 2012, 489, 414.
14. A. T. Duong, V. Q. Nguyen, G. Duvjir, V. T. Duong, S. Kwon, J. Y. Song, J. K. Lee, J. E. Lee, S. Park, T. Min, J. Lee, J. Kim, S. Cho, Nat. Commun. 2016, 7, 13713.
15. L.-D. Zhao, S.-H. Lo, Y. Zhang, H. Sun, G. Tan, C. Uher, C. Wolverton, V. P. Dravid, M. G. Kanatzidis, Nature 2014, 508, 373.
16. Y. Pei, G. Tan, D. Feng, L. Zheng, Q. Tan, X. Xie, S. Gong, Y. Chen, J.-F. Li, J. He, M. G. Kanatzidis, L.-D. Zhao, Adv. Energy Mater. 2017, 7, 1601450.
17. H. Wang, Z. M. Gibbs, Y. Takagiwa, G. J. Snyder, Energy Environ. Sci. 2014, 7, 804.
18. M.-S. Kim, W.-J. Lee, K.-H. Cho, J.-P. Ahn, Y.-M. Sung, ACS Nano 2016, 10, 7197.
19. S. A. Yamini, D. R. G. Mitchell, Z. M. Gibbs, R. Santos, V. Patterson, S. Li, Y. Z. Pei, S. X. Dou, G. J. Snyder, Adv. Energy Mater. 2015, 5, 1501047.
20. Z. Y. Li, J. F. Li, Adv. Energy Mater. 2014, 4, 1300937.
21. Q. Zhang, H. Wang, Q. Zhang, W. Liu, B. Yu, H. Wang, D. Wang, G. Ni, G. Chen, Z. Ren, Nano Lett. 2012, 12, 2324.
22. Y. Pei, A. D. LaLonde, N. A. Heinz, G. J. Snyder, Adv. Energy Mater. 2012, 2, 670.
23. X. Su, F. Fu, Y. Yan, G. Zheng, T. Liang, Q. Zhang, X. Cheng, D. Yang, H. Chi, X. Tang, Q. Zhang, C. Uher, Nat. Commun. 2014, 5.
24. Y. He, P. Lu, X. Shi, F. Xu, T. Zhang, G. J. Snyder, C. Uher, L. Chen, Adv. Mater. 2015, 27, 3639.
25. Laser-Induced Breakdown Spectroscopy (LIBS): Fundamentals and Applications Edt A.W. Miziolek, V. Palleschi, and I. Schechter, Cambridge University Press, 2006.
26. Kadel, Kamal, "Synthesis and Characterization of Thermoelectric Nanomaterials" (2014). FIU Electronic Theses and Reviews. 1170.
27. Q. H. Zhang, X. Y. Huang, S. Q. Bai, X. Shi, C. Uher, L. D. Chen, Adv. Eng. Mater. 2016, 18, 194.
28. M. Zebarjadi, K. Esfarjani, M. S. Dresselhaus, Z. F. Ren, G. Chen, Energy Environ. Sci. 2012, 5.
29. M. D. Thakor, S. K. Hadia, A. Kumar, "Precise temperature control through Thermoelectric Cooler with PID controller", presented at 2015 International Conference on Communications and Signal Processing (ICCSP), 2-4 April 2015.
30. A. Khajepour, F. Rahmani, Appl. Radiat. Isotopes 2017, 119, 51.
31. T. C. Holgate, R. Bennett, T. Hammel, T. Caillat, S. Keyser, B. Sievers, J. Electron. Mater. 2015, 44, 1814.
32. J. Yang, "Potential applications of thermoelectric waste heat recovery in the automotive industry", presented at ICT 2005 24th International Conference on

Thermoelectrics, 2005., International Conference on Thermoelectrics, ICT, 19-23 June 2005.
33. S. LeBlanc, Sustain. Mater. Technol. 2014, 1–2, 26.
34. C. K. Liu, W. K. Han, H. C. Hsieh, "Thermoelectric waste heat recovery for automotive", presented at 2014 9th International Microsystems, Packaging, Assembly and Circuits Technology Conference (IMPACT), 22-24 Oct. 2014.
35. X. Liu, Y. D. Deng, S. Chen, W. S. Wang, Y. Xu, C. Q. Su, Case Studies in Thermal Eng. 2014, 2, 62.
36. L. Rebenklau, P. Gierth, A. Paproth, K. Irrgang, L. Lippmann, A. Wodtke, L. Niedermeyer, K. Augsburg, F. Bechtold, Ieee, 2015 European Microelectronics Packaging Conference (Empc) 2015.
37. T. M. Tritt, M. A. Subramanian, Mrs. Bull. 2006, 31, 188.
38. R. M. Atta, In. J. Water Res. Arid Env. 2011, 1, 142.
39. L. Vladimir, J. Micromech. Microeng 2011, 21, 125013.
40. E. Romero, R. O. Warrington, M. R. Neuman, Physiol. Meas. 2009, 30, R35.
41. V. Leonov, R. J. M. Vullers, J. Renew. Sust. Energy 2009, 1, 062701.
42. M. S. Dresselhaus, G. Chen, M. Y. Tang, R. G. Yang, H. Lee, D. Z. Wang, Z. F. Ren, J. P. Fleurial, P. Gogna, Adv. Mater. 2007, 19, 1043.
43. G. Joshi, H. Lee, Y. Lan, X. Wang, G. Zhu, D. Wang, R. W. Gould, D. C. Cuff, M. Y. Tang, M. S. Dresselhaus, G. Chen, Z. Ren, Nano Lett. 2008, 8, 4670.
44. D.M. Rowe, “CRC handbook of thermoelectrics”, Boca Raton, 1995.
45. Lei Yang, Zhi-Gang Chen , Matthew Dargusch, and Jin Zou, Dr. L. Yang, Prof. Z.-G. Chen, Prof. M. Dargusch and Prof. J. Zou ‘High Performance Thermoelectric Materials: Progress and Their Applications’ 2017, DOI: 10.1002/(aenm.201701797).